Digest Journal of Nanomaterials and Biostructures Vol. 14, No. 2, April - June 2019, p. 479 - 490

A GREEN APPROACH FOR THE SYNTHESIS OF ANTIMICROBIAL BIO-SURFACTANT SILVER NANOPARTICLES BY USING A FERN

A. CHATTERJEE[a], S. KHATUA[c,d], K. ACHARYA[c,e], J. SARKAR[b,c,*]
[a]*Department of Botany, University of Kalyani, Kalyani, Nadia, West Bengal, India, Pin—741235.*
[b]*Department of Botany, Dinabandhu Andrews College, Garia, Kolkata, West Bengal, India, Pin—700084.*
[c]*Molecular and Applied Mycology and Plant Pathology Laboratory, Centre of Advanced Study, Department of Botany, University of Calcutta, Kolkata, West Bengal, India, Pin—700019.*
[d]*Department of Botany, Krishnagar Govt. College, Krishnagar, Nadia, West Bengal, India, Pin-741101.*
[e]*Center for Research in Nanoscience & Nanotechnology, Technology Campus, University of Calcutta, Kolkata, West Bengal, India, Pin—700098.*

Advancement of an environment-friendly, trustworthy, and speedy route for the generation of Ag-NP using natural system is an essential urge in nanotechnology. This study accounts for the efficacy of liquid extract of *Adiantum lunulatum* Burm. f. for the synthesis of Ag-NP. This is the first attempt of introducing the biosynthesis mechanism of Ag-NP using the extract of this plant along with the antimicrobial evaluation of the Ag-NP. All the detailed features of the fabricated nanoparticles were well documented by UV-Vis, DLS, Zeta Potential, FTIR, EDX, XRD, and TEM. The mean diameter of Ag-NP was about 28±2 nm. Antibacterial proficiency of Ag-NP was also determined against various gram natured pathogenic bacteria.

(Received April 4, 2019; Accepted June 14, 2019)

Keywords: Adiantum lunulatum, Biosynthesis, Silver Nanoparticles, Antimicrobial

1. Introduction

Nanotechnology is an imperative tool for the expansion of science in the present era. It is the competence to produce and design structure at nano-metric range [1] and a stimulus for the expansion of several other fields like physiochemical [2], optical [3], electrical [4], sensing [5], catalysis [6], photochemical [7], etc. due their exclusive feature of sizeable surface area to volume ratio.

Silver is one of the safe inorganic elements which is projected as “next-gen” antimicrobial agent [8]. As consequences metallic silver made an incredible response in the form of Ag-NP. This has unfolded novel strategies to use metallic silver. Ag-NP has extensive angles of application concerning bio-labeling [9], [10], antibiotics [11], antibacterial [12], [13], antifouling & anti-parasitic [14] properties, drug delivery mechanisms [15] etc. They are also highly effectual in triggering of inflammation & apoptosis than bulk silver material. It also acts as a catalyst for the reduction of dye like methylene blue [16], enhances radiation therapy [17], used in ESR dosimetry [18], glyconano sensors for diseases diagnosis [19]. But still, there are many lacunas regarding the appliance of Ag-NP on the evaluation of the risk of human health and environment and human health [20].

Various protocols are known to date for developing metallic nanoparticles. They are mainly parted into two approaches- (i) top-down and (ii) bottom up [21]. The former one defines to be a reduction in the size of bulk material by means of mechanical methods, and later one is a

*Corresponding author: jsarkar80@gmail.com

process of assembling smaller particle into a larger entity. Production of nanoparticles by chemical means is one such example [22]. However, the nanoparticles synthesized via chemical means are hazardous as for the utilization of various toxic and corrosive chemicals during the production process [23]. Moreover, the process is not so cost-effective [11]. Therefore, an urge to develop an eco-friendly and a non-hazardous route to manufacture nanoparticles which can meet both cost & energy demands [24] has become an urgent need.

Consequently, the biological performances are considered as an alternative and advancement over former approaches as it involves natural compounds such as sugars, biodegradable polymers, plants extracts [3], [25]–[28]. Metallic nanoparticles manufactured by fungi [11], [29], [30], bacteria [31], algae [27] and plants [26], [32] are well known. Furthermore, the rate of plant synthesized nanoparticles is much faster [26], [32], stable [24] and are highly mono-dispersive [33] in relation to supplementary biological methods.

Among cryptograms, the use of algae [24] & bryophytes [34] to fabricate nanoparticles are quite popular. Unlike that of pteridophytes (fern & fern allies) for forging of nanoparticles are less investigated. Till date only few of the pteridophytes like *Adiantum capillus-veneris* [35], *Adiantum caudatum* [36], *Adiantum philippense* [37], [38], *Azolla microphylla* [39], [40], *Pteris tripartita* [41], *Asplenium scolopendrium* [42], *Actinopteris radiata* [43], *Christella dentata*, *Cyclosorus interruptus*, *Nephrolepis cordifolia* [44] have been used so far.

Adiantum lunulatum Burm. f. is recognized for it's antioxidant [45], antimicrobial [46] & medicinal properties like anti-hyperglycemic action [47] against influenza and tuberculosis [48]. The plant is enriched with carbohydrates, terpenoids, phenols, and flavonoids [45], [49], [50]. These versatile features of this plant made it our choice in the first place to fulfill our goals. Thus, this current study was designed with an intention of synthesis of Ag-NP by a greener route by using the fern *Adiantum lunulatum* and assessment of the antibacterial nature of these Ag-NP against various pathogenic microorganisms.

2. Experimental

2.1. Chemicals

The chemical silver nitrate ($AgNO_3$) was procured from Sigma, St. Louis, MO, USA.

2.2. Plant material

The plant was collected from different areas of West Bengal like Kalyani (22.9751° N, 88.4345° E) of the district Nadia, West Bengal, Kalingpong district (27.066668° N, 88.466667° E) and Rajpur-Sonarpur Municipality area (22.4491° N, 88.3915° E) of the district South 24 Parganas, West Bengal, India. The respective plant specimen was self-identified and binomially jointly by Pteridology & Paleobotany Lab, Department of Botany, University of Kalyani, Kalyani, Nadia, West Bengal, India, Pin-741235 and Department of Botany, Dinabandhu Andrews College, Garia, Kolkata, West Bengal, India, Pin-700084. Voucher specimens were made from the collected specimen and further deposited both at the Herbarium of the Botany Department, University of Kalyani as well as Herbarium of the Botany Department, Dinabandhu Andrews College.

2.3. Preparation of plant extract

At first, the whole plant was washed entirely by tap water and distilled water respectively. The superficial water was dried from the plant body by proper desiccation. Then, 5 gm of that desiccated plant material was crushed in mortar & pestle into a paste. After that hundred ml of distilled water was mixed to that paste [37]. Filtration of the crude solution was done thrice by Whatman filter paper no.1. Finally, the filtrate was collected all together for future reference.

2.4. Synthesis of Ag-NP

Hundred ml of 1mM $AgNO_3$ solution was mixed to the liquid extract (1:5v/v) and stirred constantly for 1 hour [11], [13]. Both, positive (plant extract) and negative control ($AgNO_3$ solution only) were conserved under similar environments.

Centrifugation was followed to separate out the Ag-NP (at 12000 g for 15 min), and the settled nanoparticles were washed (three times) in deionized water. The purified Ag-NP were re-suspended in deionized water and ultra-sonicated by Piezo-u-sonic ultrasonic cleaner (Pus-60w) and kept at normal room temperature (37°C) [30].

2.5. UV–Vis absorption spectroscopy analysis

Adiantum lunulatum mediated biosynthesized nanoparticles had been observed under Hitachi 330 Spectrophotometer with plasmon peaks at varied regions of the spectral range 300 to 700 nm which resembled different signature marks for the production of different nanoparticles respectively [51], [52]. Deionized water was selected for reference.

2.6. Particle size measurement by DLS experiment

Particle size was found out by using Zen 1600 Malvern nanosize particle analyzer ranging between 0.6 nm and 6.0 μm under such conditions particle having an absorption coefficient of 0.01, particle refractive index 1.590, water refractive index 1.33, viscosity –cP, Temperature-25°C and a broad calculation model for irregular particles. About 10−15 measurement cycles of 10 s each was taken in account. The acquired data were averaged by the preloaded software (DTS, version 5.00 from Malvern) of the respective instrument [53].

2.7. Zeta potential measurement

Using Beckman Coulter DelsaTM Nano Particle Analyser (USA) zeta potential (Charge distribution) of the nanoparticles was investigated by revealing the solution with He–Ne laser in a sample cell (658 nm). Using Phase Analysis Light Scattering mode measurements were taken with an Ag electrode [54].

2.8. EDS analysis

A small amount of sample was taken in glass slide creating a reedy layer of the sample. An additional sample was blotted off and then the sample was permitted to dry for overnight [55]. Hitachi S 3400N instrument was the automatic choice for us to carry out the analysis of the samples. The spectra were recorded for future analysis.

2.9. XRD- measurement

The crystallinity of forged Ag-NP was confirmed and determined by XRD analysis. The XRD sample was all set on a microscopic glass slide by depositing the centrifuged sample and thereafter dried at 45ºC in a vacuum drying oven overnight. The vacuum dried Ag-NP were then used for powder X-ray diffraction analysis.

The diffractogram was documented from PANalytical, XPERTPRO diffractometer using Cuk (Cu Kα radiation, λ 1.54443) as X-ray source running at 45 kV and 30 mA [56]. The diffracted intensities were noted from 35° to 99° 2θ angles [53], [57], [58].

2.10. FTIR analysis

The vacuum dried inorganic metal nanoparticles were mixed up individually with KBr, alkali halide at a ratio of 1:100 (weight/weight). The two materials were then grounded to a fine powder in a mortar and pestle separately. Then the mixture was converted into a pellet press consisting of two pistons in a smooth cylindrical chamber. The pressure of up to 25000 psi was then applied for different measures of time in a vacuum. After that, the pistons were removed and the clear pellet was placed in a holder of the spectrophotometer. Since the KBr did not absorb infrared radiation in the region 4,000 and 400 cm^{-1} a complete spectrum of the solid was obtained [59]. The spectra were viewed by Shimadzu 8400S FTIR spectrophotometer. The spectral domain was set down in between four thousand and four hundred cm^{-1} [56].

2.11. TEM inspection of nanoparticles

Morphological and topographical characterization of the nanoparticles had been well established by the TEM studies [21]. On a carbon-coated copper grid thin films of the synthesized Ag-NP were prepared (30 μm × 30 μm mesh size) and a droplet of the Ag-NP suspension was

spotted on the grid. With the help of blotting paper, the excess sample was blotted off and then it was kept for drying off under a mercury lamp for five minutes. The synthesized particles were examined and visualized by TEM using a Tecnai G2 spirit Biotwin instrument (FP 5018/40), operating at around 80 kV accelerating voltage [60].

2.12. Estimation of antibacterial potentiality

Bacillus subtilis MTCC Code 736, *Listeria monocytogenes* MTCC Code 657, *Staphylococcus aureus* MTCC Code 96, *Escherichia coli* MTCC Code 68, *Klebsiella pneumoniae* MTCC Code 109 and *Salmonella typhimurium* MTCC Code 98 were obtained from MTCC, Institute of Microbial Technology, Chandigarh, India. Antibacterial nature was estimated by determining minimum inhibitory concentration (MIC) values according to the microdilution method [61], [62]. The six investigating bacteria were freshly cultured and 1×10^5 CFU/ml concentrated dilutions were constructed separately. Reactions were performed in ninety-six well plate consisting of 200 µl of NB, 20 µl of inoculum and different dilutions of polymers. Following incubation for one day at 37°C, 40 µl of INT dye (0.2 milligrams/milliliter) was mixed and incubated for the next round of thirty min. The concentration that inhibited 50% progression of bacteria growth as compared with positive control was calculated as MIC value. Streptomycin was cast-off as a standard drug.

3. Results and discussion

3.1. Characterization and identification of the plant specimen

The plant is rhizomatous, sub-erect to erect in posture, Entire body appears to be shiny and glabrous. Plant body ranges between 9–18 inches and are non-articulate (Fig. 1A). The mature stem appears to be brownish to dark in colour. Lamina is simply pinnate, lanceolate. Pinnae is finely leathery which is deep green or pale in colour, glabrous above and below, up to 10 pairs, stalked, alternate, fan-shaped (Fig. 1C) [63]–[65]. Venation pattern of the pinnae is dichotomous (Fig. 1D)[63]. Sporophylls are not grouped in strobili, whereas sporangia are enclosed in sporocarps. Sori is not dorsal and have false indusium, sporangia formed in definite groups [66]. T.S of the stem shows sclerenchymatous ground tissue and are 3–4 layered followed by parenchymatous cells. The xylem appears to be V-shaped with two arms that are turned inwards (Fig. 1B). Xylems are also both exarch and diarch [63], [67], [68]. The outer wall of spore appears to be rugulate under SEM which is an enlisted characteristic of the species [69] (Fig. E-G). Hence, the observation made from the above evidence identifies the specimen to be *Adiantum lunulatum* Burm.f. (*A. Philippense* Linn.) of the family Pteridaceae.

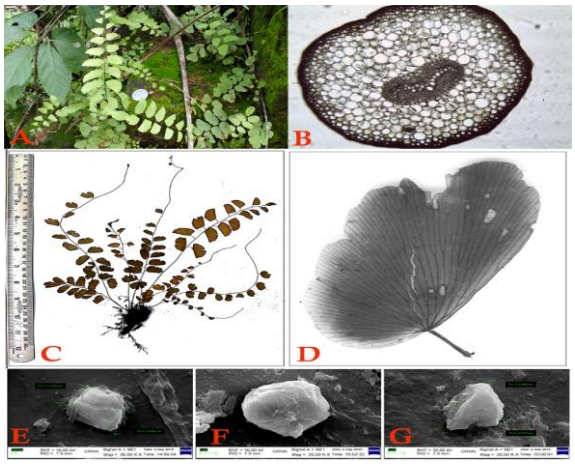

Fig. 1. (A) Digital photograph of the sporophyte of Adiantum lunulatum Burm. f. used in the biosynthesis of Ag-NP, (B) Transverse Section of the stem of Adiantum lunulatum, (C) Photograph of the Herbarium Specimen of Adiantum lunulatum Burm. f., (D) Venation pattern of the leaf of Adiantum lunulatum, (E–G) Scanning Electron Microscopic images of the spores of Adiantum lunulatum.

3.2. Production and characterization of Ag-NP

Ag-NP exhibits dark brown colour in liquid solution due to excitation of SPR in Ag-NP. Reduction of the Ag ions to Ag-NP at the time of contact to the liquid extract of *Adiantum lunulatum* could be followed by colour change. The liquid extract mediated synthesis of Ag-NP was validated by visually monitoring three flasks containing the $AgNO_3$ solution, a liquid extract of *Adiantum lunulatum* and the reaction mixture of the liquid plant extract with $AgNO_3$ solution respectively. An instantaneous and immediate turn over in the colour of the reaction mixture from colourless solution to brown colour signified the formation of Ag-NP (Fig. 2B) [70], whereas the liquid plant extract (Fig. 2A) and the $AgNO_3$ solution (Fig. 2C) were observed to retain their original colour. The colour of the control samples showed no change with cumulative incubation time. The appearance of a prominent brown colour designated the occurrence of the reaction and the development of the Ag-NP [53].

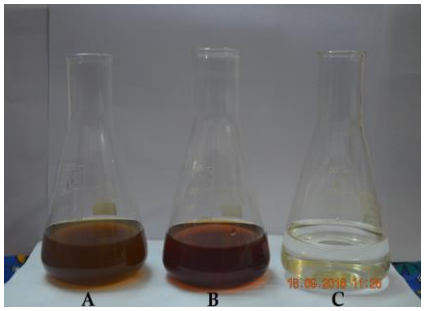

Fig. 2. Three flasks containing (A) only the liquid plant extract, (B) reaction mixture of liquid plant extract and $AgNO_3$ solution and (C) Only $AgNO_3$ solution, respectively.

3.3. UV–Visible spectroscopic analysis of Ag-NP

The evolution of silver from Ag^+ ions to Ag^0 state was categorized for spectral analysis. A broad and strong SPR band of the reaction solution was obtained in the visible spectrum at 420 nm, which was specific for Ag-NP (Fig. 3). Furthermore, this spectral analysis advocated that the Ag-NP were not in aggregated form. They scattered very well in the suspension [43], [53].

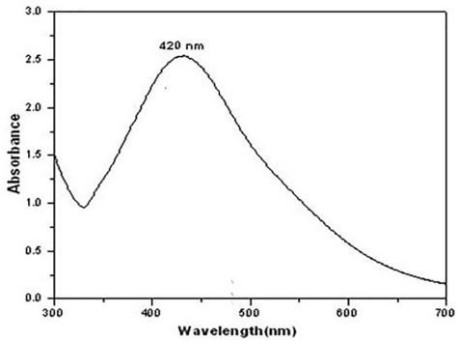

Fig. 3. UV–VIS spectrum of the synthesized silver nanoparticles.

3.4. Particle size measurement of Ag-NP

The DLS measurement was performed to get the knowledge of the size of the Ag-NP. Laser diffraction had shown that particle size found in the between 30–98 nm range (Fig. 4) The average diameter of these $AgNO_3$ nanoparticles was calculated to be 65±2 nm [71].

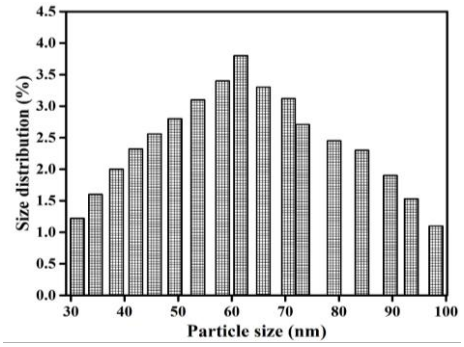

Fig. 4. The particle size distribution of bioreduced silver nanoparticles.

3.5. Zeta potential of Ag-NP

As displayed in Fig. 5, the zeta potential obtained from the Ag-NP showed a surface charge with a value of –84.11 mv [72]. The particles repel each other in suspension either having a negative or a positive zeta potential and also there shall be a very less tendency for the particles to come along. The slightly negative charge on the nanoparticles was probably resulting in the high stability of the Ag-NP without forming any aggregates when kept for an extended episode of time of more than a month [73]. Even the samples were retained their characteristic nature for more than a year (data not shown).

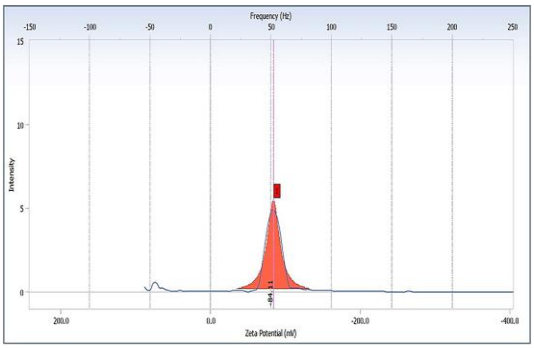

Fig. 5. Zeta potential of the biosynthesized silver nanoparticles.

3.6. EDX observation of Ag-NP

Fig. 6 illustrates the spot-profile mode of the EDX spectrum recorded from one of the densely-populated Ag-NP areas. In EDX spectra of Ag-NP, a sharp wide peak was detected in between 3–4 keV spectral region. The peak around 3–4 keV spectral region associated with the binding energies of silver [74]. The incident of that sturdy signal from Ag atoms (87.76%) itemized that the nanoparticles were solely made by silver. Therefore, EDX spectra of the Ag-NP established the presence of silver in the nanoparticles without any impurity of peaks [34]. However, there were other peaks of EDX for Cl and P, signifying that they were mixed precipitates from the plant extracts.

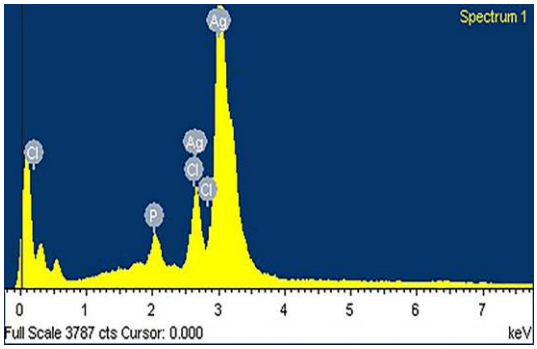

Fig. 6. EDX spectrum of silver nanoparticles.

3.7. Analyses of the crystallinity of Ag-NP by XRD

XRD measurement often proves to be a useful analytical gizmo for the identification of the crystalline nature of the newly formed compounds and their respective phases. XRD patterns of the dried Ag-NP revealed the subsistence of sharp diffraction lines at low angles (2° to 99°). The Ag-NP pointed out four sharp peaks of Ag at 2θ = 38°, 44°, 64° and 78° that could be indexed to the (111), (200), (220) and (311) facets of Ag, respectively (JCPDS card file no. 04-0783) [Fig. 7] [75]–[79]. Thus, the XRD-spectrum measurement, answered in four strong peaks agreed to the Bragg's reflection of silver nanocrystals, finalized the crystalline nature of the Ag-NP [80]. The unambiguous background noise was undoubtedly due to the shell of protein around the nanoparticles [56].

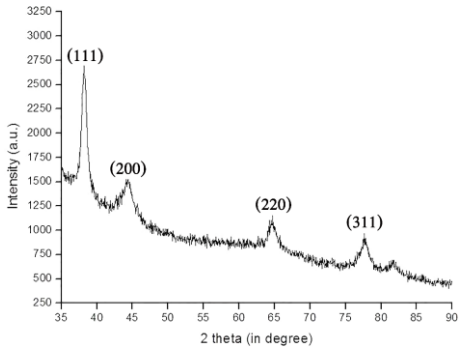

Fig. 7.XRD pattern of silver nanoparticles.

3.8. FTIR analysis of Ag-NP

FTIR absorption spectra of biosynthesized vacuum-dried Ag-NP have presented in Fig. 8. The spectra exhibited an extensive and strong absorption band corresponding to the O–H stretching vibration at around ~3,066 cm^{-1}. Symmetric and anti-symmetric modes of C–H stretching vibration were observed in the spectral region around ~2,889 cm^{-1} and ~2,820 cm^{-1} respectively [81]–[83]. Taraschewski et al. [84] reported earlier that the peak at around ~2,360 cm^{-1} was observed due to CO_2 vibration that might not be necessarily from the sample. Peaks at around ~1,567, ~1,380, and ~1,070 cm^{-1} were attributed to C=C stretching, $–NH_2$ symmetric stretch, and CO vibrations, respectively [34], [82], [85]–[87]. The band at around ~1,567 cm^{-1}, which commensurate to bending vibration movements in amides II, was earlier reported during the synthesis of Ag-NP [34]. The bands are visible in between the range of 500 to 750 cm^{-1} which confirmed the presence of R-CH group which might come from the liquid plant extract [88]. From this result, it could be stated that the soluble polypeptides present in the liquid plant extract may have acted as a capping agent to prevent the aggregation of Ag-NP in solution, and thus playing a

relevant role in their extracellular synthesis and shaping of the quasi-spherical Ag-NP [11], [30], [89].

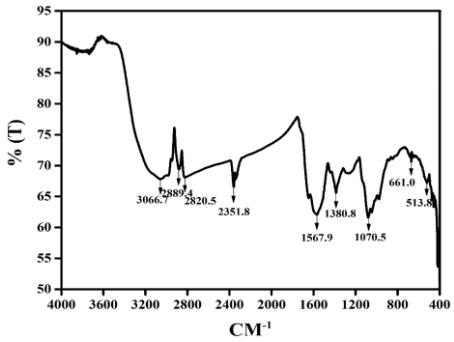

Fig. 8. FTIR absorption spectra of biosynthesized Ag-NP.

3.9. TEM of Ag-NP

TEM image, shown in Fig. 9, recorded dissimilar dimensions of Ag-NP which arose from the bio-reduction of the silver solution by liquid plant extract at room temperature (30ºC). The particles were found to be hexagonal, quasi-spherical as well as monodisperse in nature (Fig. 9 A-C) [11]. The measured diameter of these Ag-NP was in the domain of about 10–60 nm [90]. The average diameter of these Ag-NP was calculated to be 28±2 nm. The SAED pattern showed bright circular spots which further confirmed the single crystalline property of the Ag-NP (Figure 8D) [71]. It was thought-provoking to note that most of the Ag-NP in the TEM images were not in physical contact but were separated by a fairly undeviating inter-particle distance. Due to the developmental course of the sample preparation, the observed diameter of the Ag-NP during TEM analysis was quite unlike from that of the results obtained from DLS measurement as because Ag-NP were in a dry state in TEM whereas in the hydrated state in DLS experiment [91].

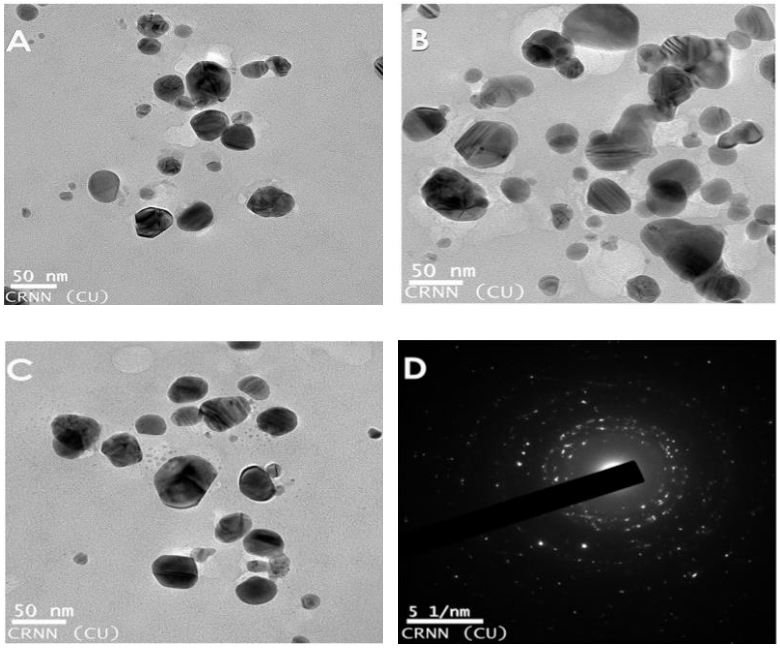

Fig. 9. (A–C) TEM images of Ag-NP (D) Selected area electron diffraction (SAED) patterns of crystalline Ag-NP.

3.10. Analysis of the effect of synthesized Ag-NP on some pathogenic bacteria

The biosynthesized Ag-NP was studied in 96 well plates for determining its antibacterial activity against both Gram-positive and Gram-negative bacteria. As presented in Table 1, the growth of all experimental strains was found to be subdued by the treatment of the Ag-NP as compared to Gram-negative control. In the case of *Listeria monocytogenes*, a Gram-positive bacterium, introduction of 25 μg/ml of Ag-NP caused 72.64±4.58% of reduction of bacterial density. Interestingly, growth of all examined Gram-negative bacteria were also noticed to be affected in the presence of a similar dose of the nanomaterials. Treatment of 25 μg/milliliter of synthesized Ag-NP showed maximum inhibition 48.45±2.87 and 88.7±5.62% with reference to *S. typhimurium* and *E. coli* respectively. These findings recommended strong antibacterial potentiality of synthesized Ag-nano.

Table 1. Antibacterial activity of synthesized silver nanoparticles as determined by the minimum inhibitory concentration value (μg/ml) (mean ± standard deviation; n = 3).

Type of bacteria	Name of bacteria	Nanoparticles	Streptomycin
Gram positive	*Listeria monocytogenes*	17.55 ± 3.57	4.68 ± 0.17
	Staphylococcus aureus	17.85 ± 1.71	6.29 ± 0.16
	Bacillus subtilis	105.41 ± 14.23	5.61 ± 0.01
Gram negative	*Escherichia coli*	12.36 ± 2.68	5.41 ± 0.11
	Salmonella typhimurium	28.77 ± 1.47	5.09 ± 0.03
	Klebsiella pneumoniae	17.84 ± 0.58	5.29 ± 0.14

4. Conclusions

The current work described biosynthesis of stable Ag-NP using liquid plant extract of *Adiantum lunulatum*. The production of biosynthesized nanomaterial was established by UV-Vis, DLS, EDX, XRD, FTIR and TEM analysis. The green synthesized Ag-NP presented strong antibacterial potentiality against pathogenic Gram-positive (*Listeria monocytogenes*, *Staphylococcus aureus*, and *Bacillus subtilis*) and Gram-negative (*Escherichia coli*, *Salmonella typhimurium* and *Klebsiella pneumoniae*) bacteria. Thus, the green synthesis of antimicrobial Ag-NP using liquid plant extract was an environment-friendly method as compared to the conventional physical and chemical synthesis techniques.

Acknowledgements

The authors thank Dr. Sudha Gupta, Assistant Professor, Pteridology & Paleobotany Lab, Department of Botany, University of Kalyani, Kalyani, Nadia, West Bengal, India, Pin-741235 for her entire effort in plant specimen identification and encouragement regarding this work. We also acknowledge Sinha Institute of Medical Science and Technology for providing us with the centrifugation and -20°C refrigeration facility.

Conflict of interest

On behalf of all listed authors, the corresponding author declares that there is not any sort of financial and non-financial conflict of interests in the subject materials mentioned in this manuscript.

References

[1] V. Filipe, A. Hawe, W. Jiskoot, Pharm. Res. **27**(5), 796 (2010).
[2] S. Galindo-Rodriguez, E. Allémann, H. Fessi, E. Doelker, Pharm. Res. **21**(8), 1428 (2004).
[3] A. Vilchis-Nestor, V. Sánchez-Mendieta, Mater. Lett. **62**(17–18), 3103 (2008).
[4] P. Magudapathy, P. Gangopadhyay, Phys. B Condens. **299**(1–2), 142 (2001).
[5] F. Frederix, J. Friedt, K. Choi, W. Laureyn, Anal. Chem. **75**(24), 6894 (2003).
[6] N. Jana, T. Sau, T. Pal, J. Phys. Chem. B **103**(1), 115 (1999).
[7] N. Chandrasekharan, P. Kamat, J. Phys. **104**(46), 10851 (2000).
[8] A. Gade, A. Ingle, C. Whiteley, M. Rai, Biotechnology Letters **32**(5), 593 (2010).
[9] M. Hayat, Colloidal gold: principles, methods, and applications. Academic Press INC, 2012.
[10] V. Filipe, A. Hawe, W. Jiskoot, Pharm. Res. **27**(5), 796 (2010).
[11] J. Sarkar et al., Dig. J. Nanomater. Biostructures **6**(2), 563 (2011).
[12] D. Maity et al., J. Appl. Polym. Sci. **122**, 2189 (2011).
[13] M. M. R. Mollick et al., Int. J. Green Nanotechnol. **4**(3), 230 (2012).
[14] S. K. Srikar, D. D. Giri, D. B. Pal, P. K. Mishra, S. N. Upadhyay, Green Sustain. Chem. **6**(1), 34 (2016).
[15] S. Mann, G. A. Ozin, Nature **382**(6589), 318 (1996).
[16] T. J. I. Edison, M. G. Sethuraman, Process Biochem. **47**(9), (2012).
[17] R. Lu, D. Yang, D. Cui, Z. Wang, L. Guo, Int. J. Nanomedicine **7**, 2101 (2012).
[18] E. J. Guidelli, A. P. Ramos, M. E. D. Zaniquelli, P. Nicolucci, O. Baffa, Radiat. Phys. Chem. **81**(3), 301 (2012).
[19] C. L. Schofield, A. H. Haines, R. A. Field, D. A. Russell, Langmuir **22**(15), 6707 (2006).
[20] V. Colvin, Nat. Biotechnol. **21**(10), 1166 (2003).
[21] G. Cao, Nanostructures and nanomaterials: synthesis, properties and applications. 2004.
[22] V. Rotello, Nanoparticles: building blocks for nanotechnology. Springer, Boston, MA, 2004.
[23] W. De Jong, P. Borm, Int. J. Nanomedicine, 2008.
[24] S. Saif, A. Tahir, Y. Chen, Nanomaterials **6**(11), 209 (2016).
[25] K. Mukunthan, S. Balaji, Int. J. Green **4**(1), 54 (2012).
[26] V. V Makarov et al., Acta Naturae **6**(1), 35 (2014).
[27] S. Iravani, "Green synthesis of metal nanoparticles using plants," Green Chem., 2011.
[28] S. S. Shankar, A. Rai, A. Ahmad, M. Sastry, J. Colloid Interface Sci. **275**(2), 496 (2004).
[29] J. Sarkar, M. Ghosh, A. Mukherjee, D. Chattopadhyay, K. Acharya, Bioprocess Biosyst. Eng. **37**(2), 165 (2014).
[30] J. Sarkar, S. Ray, D. Chattopadhyay, A. Laskar, K. Acharya, Bioprocess Biosyst. Eng. **35**(4), 637 (2012).
[31] N. Friis, P. Myers- Keith, Biotechnol. Bioeng. **28**(1), 21 (1986).
[32] S. Ahmed, M. Ahmad, B. L. Swami, S. Ikram, Journal of Advanced Research **7**(1), 17 (2016).
[33] G. Dhillon, S. Brar, S. Kaur, Crit. Rev. **32**(1), 49 (2012).
[34] K. Acharya, J. Sarkar, Int. J. Pharm. Sci. Rev. Res. **29**(1), 82 (2014).
[35] S. Santhoshkumar, K. Arts, T. Nadu, "No Title," **5**(12), 5511 (2014).
[36] A. J. De Britto, D. H. S. Gracelin, P. B. Jeya, R. Kumar, P. Molecular, T. Nadu, Int. J. Univers. Pharm. Life Sci. **2**(4), 92 (2012).
[37] D. G. Sant et al., J. Nanoparticles **2013**, 1 (2013).
[38] S. Kalita, R. Kandimalla, K. K. Sharma, A. C. Kataki, M. Deka, J. Kotoky, Mater. Sci. Eng. C **61**, 720 (2016).
[39] A. K. Jha, K. Prasad, Int. J. Nanosci. **15**(1–2), 1 (2016).
[40] B. Ch, S. Kunjiappan, C. Bhattacharjee, R. Chowdhury, Nanomed. J. **2**(1), 88 (2015).
[41] X. Baskaran, A. V. G. Vigila, T. Parimelazhagan, D. Muralidhara-Rao, S. Zhang, Int. J. Nanomedicine **11**, 5789 (2016).
[42] N. A. Şuţan, I. Fierăscu, R. C. Fierăscu, D. Ş. Manolescu, L. C. Soare, Ind. Crops Prod. **83**, 379 (2016).
[43] B. Koteswaramma, J. Kamakshamma, S. Varalaksmi, Int. J. Pharma Bio Sci. **8**(1), 121 (2017).
[44] N. John, "of the ferns Cyclosorous," **9**(2), 125 (2016).

[45] M. S. Ali, M. R. Amin, C. M. I. Kamal, M. A. Hossain, Asian Pac. J. Trop. Biomed. **3**(6), 464 (2013).
[46] M. Johnson, J. Microbiol. Exp. **4**, (41), (2017).
[47] T. Paul, B. Das, K. G. Apte, S. Banerjee, R. C. Saxena, J. Diabetes Metab. **3**(9), (2012).
[48] R. Sikarwar, B. Pathak, A. Jaiswal, Int. J. Tradit. Knowl. **7**(4), 613 (2008).
[49] C. Pan, Y. G. Chen, X. Y. Ma, J. H. Jiang, F. He, Y. Zhang, Tropical Journal of Pharmaceutical Research **10**(5), 681 (2011).
[50] M. Mithraja, J. Marimuthu, M. Mahesh, Z. Paul, Trop. Biomed. **2**(1), S40 (2012).
[51] A. Henglein, J. Phys. Chem. **97**(21), 5457 (1993).
[52] M. Sastry et al., Curr. Sci. **85**(2), 162 (2003).
[53] S. Saha, J. Sarkar, D. Chattopadhyay, S. Patra, A. Chakraborty, K. Acharya, Dig. J. Nanomater. Biostruc. **5**(4), 887 (2010).
[54] M. Behera, G. Giri, Mater. Sci. **32**(4), 702 (2014).
[55] S. M. Mukhopadhyay, Sample Preparation for Microscopic and Spectroscopic Characterization of Solid Surfaces and Films. 2003.
[56] N. Vigneshwaran, A. A. Kathe, P. V. Varadarajan, R. P. Nachane, R. H. Balasubramanya, Langmuir **23**(13), 7113 (2007).
[57] Y. Sun, Y. Xia, Science (80-.). **298**(5601), 2176 (2002).
[58] S. Pal, Y. Tak, J. Song, Appl Env. Microbiol. **73**, 1712 (2007).
[59] T. Bonnal, G. Foray, E. Prud, S. Tadier, European Journal of Environmental and Civil Engineering 1 (2017).
[60] B. Schaffer, U. Hohenester, A. Trugler, F. Hofer, Phys. Rev. B - Condens. Matter Mater. Phys. **79**(4), (2009).
[61] D. Stojković et al., Food Res. Int. **53**(1), 56 (2013).
[62] D. Stojković, J. Petrović, M. Soković, J. Glamočlija, J. Kukić-Marković, S. Petrović, J. Sci. Food Agric. **93**(13), 3205 (2013).
[63] V. G. K. L. C. V. A. Pallavi, Int J Pharm. Biol. Arch. **2**(6), 1668 (2011).
[64] D. M. Hillis, Annu. Rev. Ecol. Syst. **18**(1), 23 (1987).
[65] B. Verdcourt, "Flora of Tropical East Africa," 2002.
[66] K. U. Kramer, P. S. (Peter S. Green, and E. Götz, Pteridophytes and gymnosperms. Springer-Verlag, 1990.
[67] S. Resmi, T. Vp, S. Vk, in Kerala **2**(1), 115 (2016).
[68] A. B. Hungarica **58**(1909), 199 (2016).
[69] A. F. Tryon, B. Lugardon, Spores of the Pteridophyta, New York, NY: Springer New York, 1991, pp. 1–26.
[70] G. Singhal, R. Bhavesh, K. Kasariya, A. R. Sharma, R. P. Singh, J. Nanoparticle Res. **13**(7), 2981 (2011).
[71] M. M. R. Mollick et al., Microfluid. Nanofluidics **16**(3), 541 (2014).
[72] M. Gohel, T. Soni, L. Hingorani, A. Patel, N. Patel, Curr. Res. Drug Discov. **1**(2), 29 (2014).
[73] J. Sarkar, P. Dey, S. Saha, K. Acharya, Micro Nano Lett. **6**(8), 599 (2011).
[74] S. Kunjiappan, R. Chowdhury, C. Bhattacharjee, Front. Mater. Sci. **8**(2), 123 (2014).
[75] G. Li et al., Int. J. Mol. Sci. **13**(1), 466 (2012).
[76] K. Selvi, T. Sivakumar, Int. J. Curr. Microbiol. App. Sci. **1**(1), 56 (2012).
[77] D. R. Patil, Int. J. Res. Stud. Biosci. **3**(10), 146(2015).
[78] B. V. Bhimba, S. Gurung, S. U. Nandhini, Int. J. ChemTech Res. **7**(1), 68 (2015).
[79] K. Jyoti, M. Baunthiyal, A. Singh, J. Radiat. Res. Appl. Sci. **9**(3), 1 (2016).
[80] H. W. Lu, S. H. Liu, X. L. Wang, X. F. Qian, J. Yin, Z. K. Zhu, Mater. Chem. Phys. **81**, 104, (2003).
[81] N. Sundaramurthy, C. Parthiban, Int. Res. J. Eng. Technol. **2**(6), 332 (2015).
[82] S. Chandra, N. Chakraborty, A. Dasgupta, J. Sarkar, K. Panda, K. Acharya, Sci. Rep. **5**, 15195 (2015).
[83] R. Sanghi, P. Verma, Bioresour Technol. **100**(1), 501 (2009).
[84] M. Taraschewski, H. K. Cammenga, R. Tuckermann, S. Bauerecker, J. Phys. Chem. A **109**(15), 3337 (2005).
[85] R. M. Silverstein, F. X. Webster, D. J. Kiemle, Microchemical Journal **21**, 496 (2005).

[86] C. Y. Kim, T. Sekino, K. Niihara, J. Am. Ceram. Soc. **86**(9), 1464 (2003).
[87] Y. F. Zhang, J. X. Zhang, Q. M. Lu, Q. Y. Zhang, Mater. Lett. **60**(20), 2443 (2006).
[88] A. K. Singh, M. Talat, D. P. Singh, O. N. Srivastava, J. Nanoparticle Res. **12**, 1667 (2010).
[89] J. Sarkar, K. Acharya, Synth. React. Inorganic, Met. Nano-Metal Chem. **47**(3), 365 (2017).
[90] K. P. Bankura et al., Carbohydr. Polym. **89**(4), 1159 (2012).
[91] R. M. M. Mollick et al., RSC Adv. **4**(71), 37838 (2014).